

## EFFECT OF ADSORBED IMPURITIES ON CATALYTIC OXIDATION OF CO: A LATTICE-GAS MODEL

I.M. MRYGŁOD, I.S. BZOVSKA

UDC 530.1; 535.37  
©2007Institute for Condensed Matter Physics, Nat. Acad. Sci. of Ukraine  
(1, Svientsitskyi Str., Lviv 79011, Ukraine; e-mail: iryna@icmp.lviv.ua)

The catalytic synthesis of carbon dioxide from oxygen and carbon monoxide has been studied in the framework of the lattice model, making allowance for inactive impurities on the surface and correlations between coadsorbates. The system of equations which describes the reaction dynamics on the surface has been obtained, and its solution has been found in the mean-field approximation. The results obtained are compared with the corresponding literature data.

This work aims at studying the catalytic reaction of synthesis of carbonic acid gas (carbon oxide IV) from oxygen and carbon monoxide (carbon oxide II), taking interactions on a catalyst surface into account. Carbon monoxide is a poison gas, and its neutralization by catalytic oxidation is of great practical importance. This process is important for the solution of the problem of air purification from exhaust gases and other pollution, as well as for the purification of technological gases (for example, hydrogen) from carbon monoxide. On the other hand, the reaction of carbon monoxide oxidation

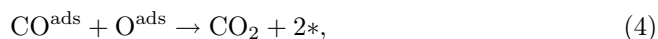


is often used as a reference one for the solution of various theoretical issues.

The kinetics of chemical oscillations in heterogeneous catalysis, in particular, in the processes of CO oxidation [1–5], has been actively studied in recent years. While simulating the reaction of CO oxidation, a suggestion is made about the dominant role of the Langmuir–Hinshelwood mechanism which provides an opportunity for the reaction to proceed provided that both reacting substances first become chemisorbed onto the surface. Nevertheless, there are several models for the scenario of this reaction. Different models account different factors that can influence the process of CO oxidation. In particular, these include such processes as diffusion [6–9] and heat transfer [7, 10], the type of the surface [11, 12], interaction between neighbors [13–15], the role of subsurface layers [16–21], the influence of the Eley–Rideal mechanism [22], surface reconstruction [23], and so on.

Theoretical researches of the kinetics of oscillatory chemical reactions of CO oxidation are based on the Ziff–Gulari–Barshad model [24]. In this work, we examine an opportunity of its generalization onto the case where the availability of inactive impurities and interactions on the catalyst surface are taken into account. Our consideration is based on the following assumptions. Suppose that the reaction proceeds only on the catalyst surface, i.e. the interaction is possible only between particles that are adsorbed on this surface. In so doing, the adsorption of an oxygen molecule occurs through the process of its fast decomposition into two atoms near the catalyst surface; each of those two atoms independently occupies a separate free active site; at the same time, carbon dioxide molecules become adsorbed onto the surface and reside there without decomposition into atoms. The transformation of particles is possible only in the adsorbed layer.

The equations of reactions that can proceed in the course of carbon monoxide oxidation on the catalyst surface look like



where the asterisk means a free active site on the catalytic surface. As a catalyst, the simple (111) surface of a Pt crystal with potassium impurities (potassium is an alkali metal which is an effective promoter in a lot of reactions that are important from the industrial point of view, such as ammonium synthesis, CO hydrogenation, and so on). Let the surface of the catalyst be simulated as a square lattice composed of  $N$  active points, each of which can be occupied by either a CO molecule or an oxygen O atom. Let us introduce the notations for the occupation numbers of the  $i$ -th site:  $n_i^1$  for adsorbed CO molecules and  $n_i^2$  for adsorbed oxygen atoms, where

$n_i^l = [0, 1]$ . The condition  $n_i^1 + n_i^2 \leq 1$  must be satisfied at that. The characteristic feature of the reaction is that the diffusion rates of CO and O differ very much from each other, because CO molecules are very mobile on the surface in comparison with the adsorbed oxygen atoms which are practically immovable. Therefore, one should distinguish between two different cases of high or low reaction rates.

In the case where the rates of adsorption and desorption of CO are higher than the rate of CO oxidation on the surface, a slow variation of the surface coverage by oxygen is described by some kinetic equation. Considering this process, we also take into account the interaction

$$H = -(\mu_1 + h_1) \sum_i n_i^1 - (\mu_2 + h_2) \sum_i n_i^2 + w_1 \sum_{\langle i,j \rangle} n_i^1 n_j^1 + w_2 \sum_{\langle i,j \rangle} n_i^2 n_j^2 + \varepsilon_{12} \sum_{\langle i,j \rangle} n_i^1 n_j^2 \quad (5)$$

between the nearest neighbors in the adsorbate, where  $\mu_1$  and  $\mu_2$  are the chemical potentials of adsorbed CO and O, respectively; and  $w_1$ ,  $w_2$ , and  $\varepsilon_{12}$  are the energies of interaction between the nearest neighbors composing the pairs CO–CO, O–O, and CO–O, respectively. To take the influence of the alkali metal on the surface properties into consideration, the fields  $h_1$  and  $h_2$  were introduced. The local energy of CO varies by  $\delta\varepsilon_1 = \widetilde{h}_1 \langle n_{\text{alkali}} \rangle = -h_1$  owing to long-range electrostatic interactions between CO and the atoms of alkali metal K ( $n_{\text{alkali}}$  means the surface covered with potassium). Similarly, the variation of the local energy of oxygen is  $\delta\varepsilon_2 = \widetilde{h}_2 \langle n_{\text{alkali}} \rangle = -h_2$ .

Such a model was proposed in work [15]. It was shown there that the kinetic phase diagrams ( $p_{\text{CO}}, 1/T$ ) contain a bistable section in the cluster approximation. It is known that various jumps from one stable branch onto the other are possible in the bistable state of the system. Provided that the system depends on a parameter which slowly varies in time, the relaxation oscillations emerge in it. In this work, we consider such a model in the mean-field approximation and will demonstrate that the interval of bistability also exists in this simpler approximation.

Consider the Hamiltonian of the system in the mean-field approximation. In this approximation, actual interactions between particles are replaced by the action of an averaged field on every particle, with the strength of the field being independent of the particle's location and its nearest environment. To pass to the mean-field approximation, we should make the

following substitutions for the occupation numbers in the Hamiltonian:

$$n_i^1 = \langle n^1 \rangle + \Delta n_i^1, \quad (6)$$

$$n_i^2 = \langle n^2 \rangle + \Delta n_i^2. \quad (7)$$

Here,  $\langle n^l \rangle = \langle n_i^l \rangle$  are the average values of the numbers  $n_i^l$  which, owing to the equivalence of all sites in the crystal lattice, do not depend on the site number. The mean-field approximation consists in neglecting the summands that are quadratic with respect to the deviations  $\Delta n_i^l$ . Therefore, such substitutions bring about the relations

$$w_1 \sum_{i,j} n_i^1 n_j^1 \simeq -w_1 N \langle n^1 \rangle^2 + 2w_1 \langle n^1 \rangle \sum_i n_i^1, \quad (8)$$

$$w_2 \sum_{i,j} n_i^2 n_j^2 \simeq -w_2 N \langle n^2 \rangle^2 + 2w_2 \langle n^2 \rangle \sum_i n_i^2, \quad (9)$$

$$\varepsilon_{12} \sum_{i,j} n_i^1 n_j^2 \simeq -\varepsilon_{12} \langle n^1 \rangle \langle n^2 \rangle N + \varepsilon_{12} \langle n^2 \rangle \sum_i n_i^1 + \varepsilon_{12} \langle n^1 \rangle \sum_i n_i^2. \quad (10)$$

As a result, the Hamiltonian of the system in the mean-field approximation looks like

$$H = -\widetilde{\mu}_1 \sum_i n_i^1 - \widetilde{\mu}_2 \sum_i n_i^2 + AN, \quad (11)$$

where the following notations were introduced:

$$A = -w_1 \langle n^1 \rangle^2 - w_2 \langle n^2 \rangle^2 - \varepsilon_{12} \langle n^1 \rangle \langle n^2 \rangle, \quad (12)$$

$$\widetilde{\mu}_1 = \mu_1 + h_1 - 2w_1 \langle n^1 \rangle - \varepsilon_{12} \langle n^2 \rangle, \quad (13)$$

$$\widetilde{\mu}_2 = \mu_2 + h_2 - 2w_2 \langle n^2 \rangle - \varepsilon_{12} \langle n^1 \rangle. \quad (14)$$

Hence, this Hamiltonian depends on the occupation numbers  $n_i$  in the same way as does the Hamiltonian of a system of noninteracting particles embedded into an external force field. Therefore, the Hamiltonian of our system is the sum of one-particle Hamiltonians, owing to which the grand partition function becomes split into the product of one-particle grand partition functions

$$\Xi_M = \prod_{i=1}^N \xi_i, \quad (15)$$

where

$$\xi_i = \sum_{n_i=0}^l \exp\left(-\frac{A - \tilde{\mu}_1 n_i^1 - \tilde{\mu}_2 n_i^2}{kT}\right) = e^{-\frac{A}{kT}} \left(1 + e^{\frac{\tilde{\mu}_1}{kT}} + e^{\frac{\tilde{\mu}_2}{kT}}\right). \quad (16)$$

The one-particle grand partition function does not depend on the site number, because all the sites are identical. Therefore, the grand partition function of the whole system is equal to

$$\Xi = \xi_1^N = e^{-\frac{AN}{kT}} \left(1 + e^{\frac{\tilde{\mu}_1}{kT}} + e^{\frac{\tilde{\mu}_2}{kT}}\right)^N, \quad (17)$$

whence we obtain the following expression for the grand thermodynamic potential:

$$\Omega = -kT \ln \Xi = -Nw_1\theta_1^2 - Nw_2\theta_2^2 - \varepsilon_{12}\theta_1\theta_2N - kTN \ln \left[1 + \exp\left(\frac{\tilde{\mu}_1}{kT}\right) + \exp\left(\frac{\tilde{\mu}_2}{kT}\right)\right]. \quad (18)$$

Making use of this formula, we can calculate all the thermodynamic functions of the system in the mean-field approximation.

Taking advantage of the thermodynamic formula

$$\theta_i = -\frac{1}{N} \left(\frac{\partial \Omega}{\partial \mu_i}\right)_T, \quad (19)$$

we obtain the following system of equations for the coverages  $\theta_i$ :

$$\theta_1 = \frac{\exp\left(\frac{\tilde{\mu}_1}{kT}\right)}{1 + \exp\left(\frac{\tilde{\mu}_1}{kT}\right) + \exp\left(\frac{\tilde{\mu}_2}{kT}\right)}, \quad (20)$$

$$\theta_2 = \frac{\exp\left(\frac{\tilde{\mu}_2}{kT}\right)}{1 + \exp\left(\frac{\tilde{\mu}_1}{kT}\right) + \exp\left(\frac{\tilde{\mu}_2}{kT}\right)}. \quad (21)$$

Those equations for  $\theta_i$  are self-consistent, because the average value of the coverage is a parameter of the distribution function, which is used to calculate the average.

In work [15], two cases, which correspond to the conditions of high and low reaction rates, were examined. Let us consider them separately. In the case where the reaction rate is low, the CO distribution is equilibrium, provided that the rate of CO diffusion is high. On

the other hand, since the adsorbed oxygens are not in equilibrium, the evolution of the oxygen coverage in time is determined by the kinetic equation

$$\frac{d\theta_O}{dt} = 2p_{O_2}k_Os_O(1 - \theta_{CO} - \theta_O)^2 - k\theta_{CO}\theta_O. \quad (22)$$

The first term describes the oxygen chemisorption onto surface-lattice sites, while the second one is associated with the reaction of CO oxidation;  $p_{O_2}$  is the partial pressure of oxygen,  $k_O$  is the frequency of collisions of oxygen molecules with the surface, and  $s_O$  is the so-called sticking factor. The parameter  $k$  characterizes the reaction rate:  $k = k_{CO_2} \exp(-\beta E_0)$ , where  $E_0$  is the reaction activation energy. The adsorption of oxygen is dissipative; the rate of desorption is therefore very low, and it can be neglected. To analyze the stable states of such a model system, it is necessary to solve the equation  $d\theta_O/dt = 0$  together with Eqs. (20) and (21) and to find the average coverages for CO and oxygen.

In the case where the reaction rate is higher than the rates of CO adsorption and desorption, the magnitude of the CO coverage is analyzed using the kinetic equation which takes into account the processes of CO adsorption and desorption, as well as the reaction of oxidation. The evolution of the CO coverage is described by the equation

$$\frac{d\theta_{CO}}{dt} = p_{CO}k_{CO}s_{CO}(1 - \theta_{CO} - \theta_O) - d\theta_{CO} - k\theta_{CO}\theta_O, \quad (23)$$

where  $d = d_0 \exp(-\beta E_d)$  is the rate of CO desorption. Suppose that the local equilibrium distribution of CO results from the high rate of its diffusion. Then, in order to analyze the stable states, it is necessary to solve the equations  $d\theta_O/dt = 0$  and  $d\theta_{CO}/dt = 0$  together with Eqs. (20) and (21) with respect to the average coverages for CO and oxygen. Moreover, in order to analyze the dependences of the coverages of both reacting adsorbates on  $p_{CO}$ , one may assume that CO gas is ideal near the surface and apply the following relation between the partial pressure and the chemical potential:  $p_{CO} = (kT)^{5/2}(m_{CO}/2\pi\hbar^2)^{3/2} \exp[(\mu_1 - \Delta\varepsilon_1)/kT]$ , where  $m_{CO}$  is the mass of a CO molecule. An extra parameter  $\Delta\varepsilon_1$  appeared because of the differences between the chemical potentials and one-particle energies in the gaseous and adsorbed states. The value of  $\Delta\varepsilon_1$  can be found from experimental data.

First, consider the case of low reaction rate. Our purpose is to study the average coverages of CO and

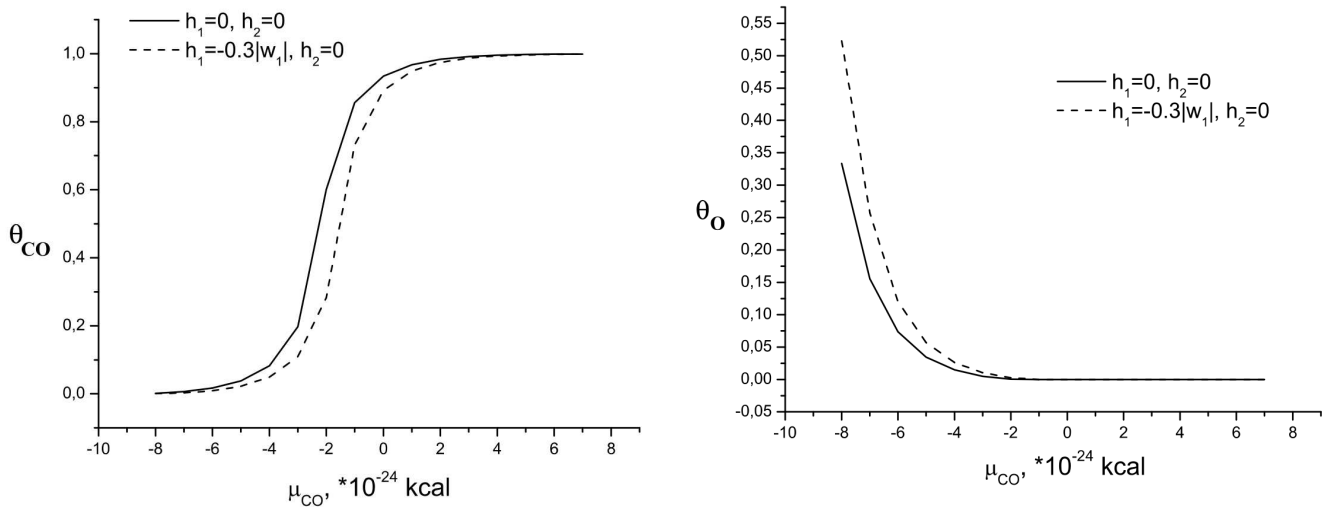


Fig. 1. Average coverages with CO (a) and oxygen (b) at  $T = 466$  K as the functions of  $\mu_{CO}$

O, as well as their dependences on  $\mu_{CO}$ . Figure 1 illustrates both the dependences obtained in the case where impurities are available on the surface ( $h_1/|w_1| = -0.3$  and  $h_2 = 0$ ) and the dependences corresponding to the case of the Pt surface without alkali metal. The following model parameters were chosen:  $E_0 = 8.2$  kcal/mol,  $\varepsilon_{12} = 1.72$  kcal/mol, and  $w_1 = -1.32$  kcal/mol, i.e. the assumption was made that the interaction in CO–O pairs is repulsive and that in CO–CO pairs is attractive by character. The values of the other model parameters were as follows:  $k_{CO_2} = 3 \times 10^6$  s $^{-1}$ ,  $k_O = 7.8 \times 10^5$  Torr $^{-1}$ , and  $s_O = 0.06$ , which corresponded to Pt(111) surface.

As is seen from Fig. 1, taking the impurities of an alkali metal into account corresponds to the increase of the local CO energy by  $\delta\varepsilon_1 = -h_1$ , which gives rise to the delocalization of adsorbed CO and, as a result, to the CO coverage reduction.

Despite the absence of the localized field ( $h_2 = 0$ ), the CO coverage reduction is accompanied by a substantial growth of the O coverage in comparison with the case  $h_1 = h_2 = 0$ . Hence, on the one hand, the long-range fields caused by alkali metal atoms bring about the CO delocalization with the corresponding reduction of the CO coverage. On the other hand, this process is accompanied by the adsorption of oxygen and the corresponding increase of the oxygen coverage.

In the case of high reaction rates, the model parameters were determined by fitting the theoretical results obtained in the framework of the cluster approximation [15] to experimental data. The following values were used:  $\varepsilon_{12} = 1.9$  kcal/mol,  $w_1 = -1.27$

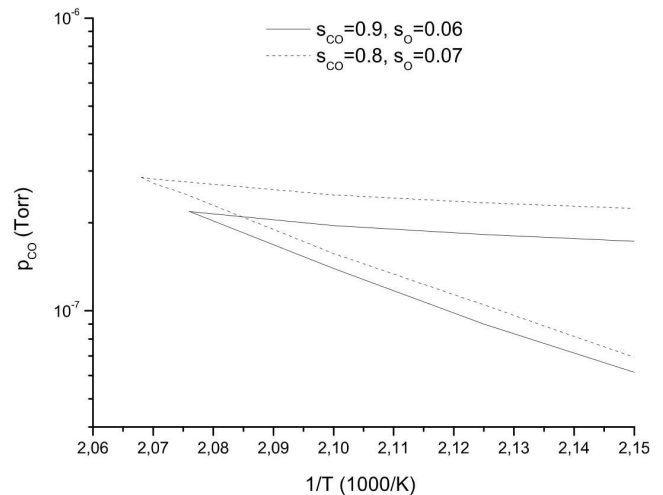


Fig. 2. Phase diagrams ( $p_{CO}, 1/T$ ) for various values of  $s_{CO}$  and  $s_O$

kcal/mol,  $E_0 = 7.9$  kcal/mol,  $E_d = 36$  kcal/mol,  $k_{CO} = 7 \times 10^6$  s $^{-1}$  Torr $^{-1}$ ,  $d_0 = 2 \times 10^{16}$  s $^{-1}$ , and  $s_{CO} = 0.9$ . The quoted values evidence for the attraction in the CO–CO pair. By analogy with the previous case (a low reaction rate), the influence of the alkali metal was taken into account by introducing the electrostatic fields  $h_1$  and  $h_2$ . In addition, according to the known experimental results, we can make allowance for the variation of the sticking factors for CO and oxygen, which is caused by the presence of alkali metal atoms. The corresponding phase diagram is depicted in Fig. 2 in two cases:  $s_{CO} = 0.9, s_O = 0.06$  and  $s_{CO} = 0.8, s_O = 0.07$ .

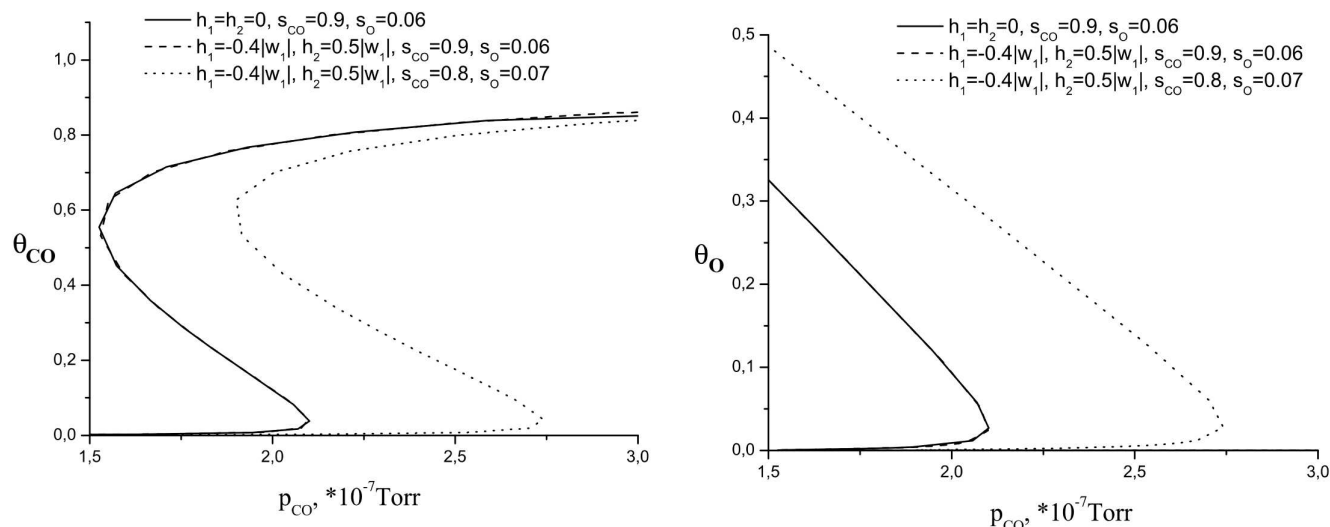


Fig. 3. Average CO (a) and oxygen (b) coverages as the functions of  $p_{\text{CO}}$  at  $T = 466$  K and for various values of the parameters  $h_1$ ,  $h_2$ ,  $s_{\text{CO}}$ , and  $s_{\text{O}}$

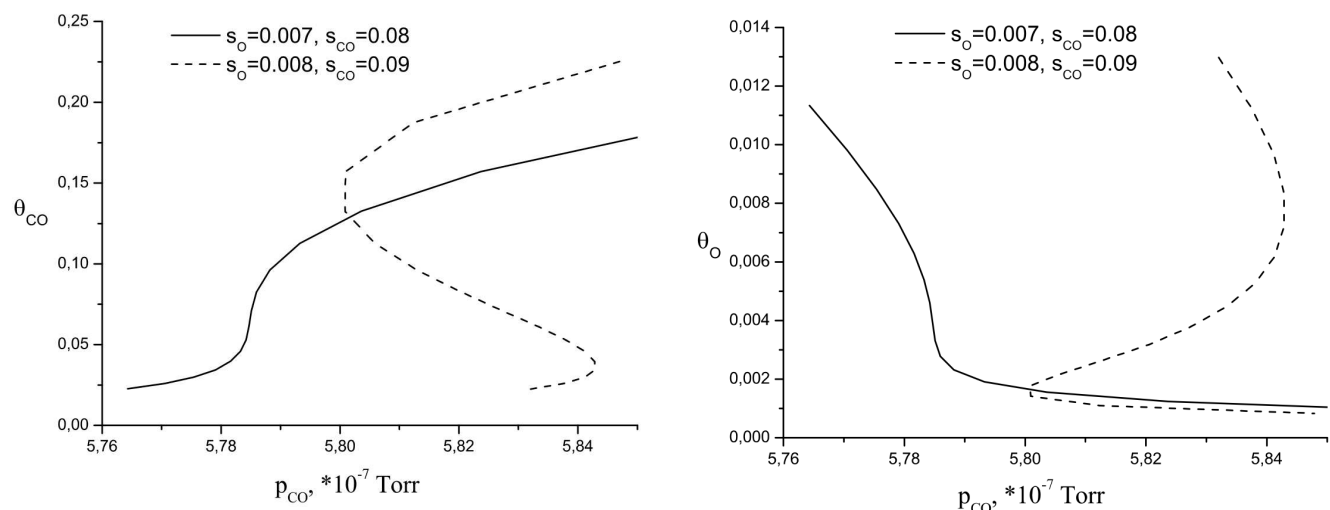


Fig. 4. Average CO (a) and oxygen (b) coverages as the functions of  $p_{\text{CO}}$  at  $T = 466$  K and for various values of the parameters  $s_{\text{CO}}$  and  $s_{\text{O}}$

It is evident from Fig. 2 that the character of solutions changes at high reaction rates: a bistable region appears. It means that the bifurcation of the solution can be observed even in the mean-field approximation. Notice that the bistable region is shifted towards higher  $p_{\text{CO}}$  pressures in the case  $s_{\text{CO}} = 0.8$  and  $s_{\text{O}} = 0.07$ .

An important characteristic feature of the results obtained is the fact that a simple account of the electrostatic fields  $h_1$  and  $h_2$  does not practically change the region of bistability, whereas the variation of the sticking factors gives rise to its significant shift. It is clearly seen from Fig. 3, where the dependences of the

CO and O coverages on the pressure  $p_{\text{CO}}$  are exhibited for various sets of sticking factors.

It is also interesting to find, in the same approximation, the lower bounds for the sticking factors  $s_{\text{CO}}$  and  $s_{\text{O}}$ , at which the region of bistability still exists. Figure 4 demonstrates that  $s_{\text{CO}} = 0.09$  and  $s_{\text{O}} = 0.008$  are those critical values, at which the bifurcation of the solution is still observed. At lower values of  $s_{\text{CO}}$  and  $s_{\text{O}}$ , the region of bistability disappears.

Therefore, the variations of  $s_{\text{CO}}$  and  $s_{\text{O}}$ , which are caused by the presence of alkali metal atoms, play an important role in the case of high reaction rates. Similarly to the previous case (the case with a slow

reaction), the shift of the diagram, which takes place if the impurities of an alkali metal are taken into account, is also accompanied by a reduction of the CO coverage and an increase of the oxygen one, which is in agreement with experimental results.

As seen, in spite of the fact that the model used is simplified and does not consider some effects, and the influence of alkali impurities is made allowance for only through introducing the long-range electrostatic fields  $h_l$  and allowing the sticking factors  $s_l$  to vary, it describes the characteristic features of the reaction of carbon monoxide oxidation on a surface rather well. It is worth noting that the region of bistability, which is observed in the cluster approximation, exists also in the mean-field approximation in the case where the reaction rate is considerably higher than that of the CO adsorption-desorption process. If the reaction rate is low, the bifurcation of solutions is not observed in this approximation. In the case of a high reaction rate, the diagram becomes shifted, first of all, owing to the variation of the sticking factors caused by the influence of the alkali metal. Concerning the variation of the electrostatic fields  $h_l$ , the results of calculations of the bifurcation point turned out almost insensible. Despite a strong CO–O repulsion, the CO delocalization is accompanied by the increase of the oxygen coverage.

1. V.P. Zhdanov, Surf. Sci. **500**, 966 (2002).
2. H. Levine and X. Zou, Phys. Rev. E **48**, 50 (1993).
3. F. Chavez, L. Vicente, A. Perera, and M. Moreau, J. Chem. Phys. **109**, 8617 (1998).
4. C.D. Lund, C.M. Surko, M.B. Maple, and S.Y. Yamamoto, J. Chem. Phys. **108**, 5565 (1998).
5. Yu. Suchorski, J. Beben, R. Imbihl, E.W. James, Da-Jiang Liu, and J.W. Evans, Phys. Rev. B **63**, 165417 (2001).
6. B.C.S. Grandi and W. Figueiredo, Phys. Rev. E **65**, 036135 (2002).
7. O. Nekhamkina, R. Digilov, and M. Sheintuch, J. Chem. Phys. **119**, 2322 (2003).
8. M. Ehsasi, M. Matloch, O. Frank, J.H. Block, K. Christmann, F.S. Rys, and W. Hirschwald, J. Chem. Phys. **91**, 4949 (1989).

9. J.W. Evans, J. Chem. Phys. **98**, 2463 (1993).
10. Y. Cisternas, Ph. Holmes, I.G. Kevrekidis, and X. Li, J. Chem. Phys. **118**, 3312 (2003).
11. N.V. Peskov, M.M. Slinko, and N.I. Jaeger, J. Chem. Phys. **116**, 2098 (2002).
12. P. Meakin and D.J. Scalapino, J. Chem. Phys. **87**, 731 (1987).
13. F. Bagnoli, B. Sente, M. Dumont, and R. Dagonnier, J. Chem. Phys. **94**, 777 (1991).
14. J. Satulavsky and E.V. Albano, J. Chem. Phys. **97**, 9490 (1992).
15. N. Pavlenko, P.P. Kostrobij, Yu. Suchorski, and R. Imbihl, Surf. Sci. **489**, 29 (2001).
16. K.M. Khan, K. Yaldram, J. Khalifeh, and M.A. Khan, J. Chem. Phys. **106**, 8890 (1997).
17. K.M. Khan and N. Ahmad, Physica A **280**, 391 (2000).
18. K.M. Khan and K. Yaldram, Surf. Sci. **445**, 186 (2000).
19. K.M. Khan, Surf. Sci. **470**, 155 (2000).
20. N. Ahmad and K.M. Khan, Chem. Phys. **263**, 339 (2001).
21. F. Chavez, L. Vicente, and A. Perera, J. Chem. Phys. **113**, 10353 (2000).
22. P. Meakin, J. Chem. Phys. **93**, 2903 (1990).
23. R. Imbihl and G. Ertl, Chem. Rev. **95**, 697 (1995).
24. R.M. Ziff, E. Gulari, and Y. Barshad, Phys. Rev. Lett. **56**, 2553 (1986).

Received 20.10.06.

Translated from Ukrainian by O.I. Voitenko

#### ВПЛИВ АДСОРБОВАНИХ ДОМІШОК НА КАТАЛІТИЧНЕ ОКИСЛЕННЯ СО: МОДЕЛЬ ҐРАТКОВОГО ГАЗУ

*I.M. Мриглюд, I.C. Бзовська*

#### Резюме

В рамках ґраткової моделі досліджено каталітичну реакцію синтезу вуглекислого газу з кисню та чадного газу (оксиду вуглецю II) із врахуванням присутності неактивних домішок і взаємодій на поверхні. Отримано систему рівнянь, що описує динаміку реакцій на поверхні каталізатора, та знайдено її розв'язки у наближенні середнього поля. Отримані результати проаналізовано і порівняно з результатами, відомими в літературі.